

Tunable Nb superconducting resonators based upon a Ne-FIB-fabricated constriction nanoSQUID

O. W. Kennedy,¹ J. Burnett,^{1,2} J. C. Fenton,¹ N. G. N. Constantino,¹
P. A. Warburton,^{1,3} J. J. L. Morton,^{1,3} and E. Dupont-Ferrier^{1,4}

¹*London Centre for Nanotechnology, UCL, 17-19 Gordon Street, London, WC1H 0AH, UK*

²*Microtechnology and Nanoscience, Chalmers University of Technology, SE-41296 Gothenburg, Sweden.*

³*Dept. of Electronic and Electrical Engineering, UCL, London, WC1E 7JE, UK*

⁴*Department de Physique, Institut Quantique, Université de Sherbrooke,
2500 Boulevard de l'Université, Sherbrooke, Quebec J1K 2R1, Canada*

(Dated: January 8, 2019)

Hybrid superconducting–spin systems offer the potential to combine highly coherent atomic quantum systems with the scalability of superconducting circuits. To fully exploit this potential requires a high quality-factor microwave resonator, tunable in frequency and able to operate at magnetic fields optimal for the spin system. Such magnetic fields typically rule out conventional Al-based Josephson junction devices that have previously been used for tunable high- Q microwave resonators. The larger critical field of niobium (Nb) allows microwave resonators with large field resilience to be fabricated. Here, we demonstrate how constriction-type weak links, patterned in parallel into the central conductor of a Nb coplanar resonator using a neon focused ion beam (FIB), can be used to implement a frequency-tunable resonator. We study transmission through two such devices and show how they realise high quality factor, tunable, field resilient devices which hold promise for future applications coupling to spin systems.

I. INTRODUCTION

A large and growing variety of spin systems have been coupled to superconducting resonators, including ensembles of non-interacting spins in silicon [1], diamond [2] and other materials [3], magnons in ferrimagnets [4] and chiral magnetic insulators [5], and individual spins in quantum dot devices [6]. Motivations for such studies include long-range coupling of spin qubits [7], realisation and study of topological systems [8], long-lived microwave quantum memories for superconducting qubits [9, 10], and the demonstration of microwave-to-optical conversion at the single-photon level [11]. Planar superconducting circuits provide a robust, well-studied [12] and scalable architecture [13] for such hybrid systems, and superconducting resonators with Q -factors over 1 million have been achieved [14]. However, for the majority of the applications described above, externally applied magnetic fields from ~ 10 mT up to several 100 mT, or more, are required to bring the spin systems into a suitable regime of interest. Furthermore, control of the spin-resonator coupling is required, often on short timescales, in applications such as quantum memories, and may be achieved, for example, by frequency-tuning of the resonator.

Superconducting quantum interference devices (SQUIDs) act as flux-tunable inductors and have been successfully incorporated into resonators to provide frequency tunability [15–17]. The SQUID inductance is tuned from its minimum to its maximum by a change of half a flux quantum in the flux threading the SQUID loop, thus altering the resonator frequency. This means that small local fields provided by on-chip flux lines are able to tune SQUID-embedded resonators on

timescales of a few nanoseconds [16]. Technologies which use DC currents to tune the kinetic inductance and hence resonant frequency of resonators have also been developed [18, 19] and coupled to spin ensembles [2]. Previous SQUID-tunable devices have been fabricated from aluminium with shadow-evaporated junctions [16] or used Nb/Al/AlO_x/Nb trilayer junctions [15]. Al devices may suffer from the low critical field of Al and are expected to have poor magnetic-field resilience. AlO_x tunnel junctions may introduce extra losses to resonators and limit quality factors. An alternative technology is based on nanoSQUIDs [20, 21] formed by superconducting-nanowire-based constriction junctions; these have already been shown to possess exceptional field resilience [22].

NanoSQUIDs are commonly fabricated [23] by a Ga-based focused ion beam (FIB); however, this technique has been shown to induce loss into superconducting resonators [24]. Here, we use a neon FIB (a technique shown to be compatible with high quality superconducting resonators [25]) to create constrictions in the central conductor of a Nb superconducting $\lambda/4$ co-planar resonator. These constrictions have a width of 50 nm and are placed in parallel such that they complete a superconducting loop between the current antinode of the resonator and the ground (Fig. 1). We study the microwave transmission of two such devices fabricated from Nb films of different quality as determined by measuring the quality of bare resonators fabricated from the same films. One such device includes a lumped element inductor which reduces the tunability of the resonator but may also be used to couple more strongly to spins in future experiments. We demonstrate that nanoSQUID-embedded resonators may realize high-quality, frequency-tunable and field-resilient resonators.

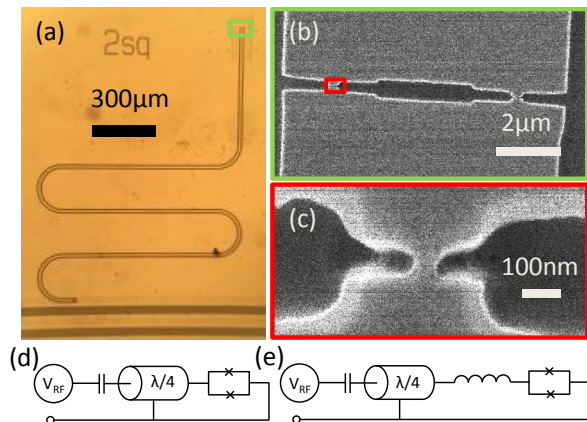


Figure 1. (a) Optical micrograph of resonator ATune (see text) with the microwave feedline shown at the bottom. The green rectangle indicates the location of (b), a He FIB micrograph, collected using an electron flood gun, showing the SQUID loop at the grounded end of ATune. The red rectangle indicates the location of (c) Ne-FIB-milled constriction with a width of 50 nm. In (a), (b) and (c), the lighter tones show the Nb and the darker tones the Si. (d, e) Equivalent circuit diagrams of the tunable resonators for (d) ATune and (e) BTune. The lumped element inductor is present in BTune and not in ATune.

II. EXPERIMENTAL

Co-planar resonators were fabricated by etching thin films of superconductor using a similar method to that described in Ref [25]. Here Nb is used, instead of NbN, because of its longer coherence length of 38 nm [26] which sets the lengthscale for the width of constrictions needed to make junctions — Nb thus allows ≈ 50 nm constrictions to be used, which is easier to achieve than the ≈ 20 nm constrictions required in NbN. Nb also has a lower kinetic inductance (hence lower impedance and larger zero-point current fluctuations), which could enable stronger magnetic coupling of the Nb resonator to spins. Nb films were deposited on Si substrates by DC magnetron sputtering from a 99.99%-pure elemental Nb target in argon. The pressure before deposition was 6×10^{-7} mbar and during deposition was 3.5×10^{-3} mbar. The sputter power was 200 W, with the deposition timed to produce a 50-nm-thick film.

Two chips are fabricated from Nb films deposited according to the same recipe in separate sputter runs and labelled A and B. We discuss two resonators from each of these chips, one tunable and one bare resonator labelled Tune and Bare respectively. We refer to resonators by a combination of chip And resonator label e.g. ATune is the tunable resonator from chip A. chip A (B) has an area of 58 mm² (44 mm²). Before deposition, chip B is dipped into HF for ~ 10 s to remove a native oxide coating and then loaded into the sputter system and put under vacuum within 5-10 minutes. Quarter-wave ($\lambda/4$) res-

onators (see Fig. 1a) with an embedded superconducting loop at the grounded end of the resonator were patterned by electron beam lithography (EBL) (Fig. 1b) in the same lithography step as a microwave feed line. The resist pattern was transferred into the film by a reactive ion etch (RIE) process using a 2:1 ratio of SF₆ to Ar, at 30 mbar and 30 W for 120 s. The RIE process additionally etches exposed Si to a depth of 500 nm, leaving areas with Nb raised above their surroundings. Resonators on chip B have a long constriction (100 $\mu\text{m} \times 1 \mu\text{m}$) embedded into the central conductor just before the SQUID. The narrow constriction create larger local fluctuating fields and increase the resonator coupling to spins in future devices [1]. The increased coupling comes at the cost of including a constriction which acts as a lumped element inductor reducing the inductance ratio between SQUID and resonator, which consequently reduces the resonator tunability.

The superconducting loop has two constrictions (see Fig. 1b and c): broad constrictions are defined in the initial EBL exposure and subsequently narrowed to ≈ 50 nm by Ne FIB milling, in which a beam of Ne ions, accelerated to 15 kV, mills through the Nb. A dose of $\approx 2 \text{ nC}\mu\text{m}^{-2}$ is used. Circuit diagrams of these devices are shown in Fig. 1 d (e) for ATune (BTune). On chip A, 21 out of 22 constrictions milled were still intact after narrowing to a dimension approaching the coherence length, suggesting a high yield for this part of the processing; see supplementary materials [27] for statistical analysis on junction widths.

Resonators are measured at a temperature $T \approx 300$ mK in a ³He cryostat with a heavily attenuated microwave in-line and a cryogenic high-electron-mobility transistor (HEMT) amplifier on the microwave out-line. The S_{21} transmission of microwaves through the feedline—to which the resonator is capacitively coupled—is measured using a Rohde & Schwarz ZNB8 vector network analyzer. Perpendicular magnetic fields are applied by a superconducting magnet connected to a precision current source (Keithley 2400 SourceMeter). Samples are enclosed in a brass box lined with Eccosorb CR-117, a microwave absorber, to reduce the number of quasiparticles excited by stray IR photons, which we have previously shown can have a significant effect on superconducting constrictions [25].

III. RESULTS

We first characterize the zero-field characteristics of the resonators on the two chips at the base temperature of the cryostat. In Fig. 2, we show the zero-field magnitude response of S_{21} from ATune (Fig. 2 a) and BTune (Fig. 2 c) at an applied power of ~ -106 dBm. Using a traceable fit routine [28], based on fitting a circle to the resonance in the real-imaginary plane, we extract the resonator parameters (fits shown in red in Fig. 2). At an applied power of ~ -106 dBm ATune, ABare, BTune

and BBare have internal quality factors $Q_i = 2.8 \times 10^4$, 5.3×10^4 , 1.25×10^5 and 1.26×10^5 respectively (resonance notches of bare resonators are not shown). The biggest difference between zero-field quality factors is between the different films rather than between the bare and tunable resonators. This shows that at high drive power, the SQUIDs introduce minimal extra losses and that the losses are dominated by effects arising from the film quality. The asymmetry of the resonance of ATune (Fig. 2a, b) persists down to single-photon powers due to an impedance mismatch and this is fully captured by the fit routine. Fig. 2b, d shows that both ATune and BTune resonances are present at applied perpendicular fields approaching 0.5mT with resonance responses. We discuss resonator behaviour in an applied magnetic field later in the manuscript.

We measure the internal losses of all four resonators ($\delta_i = 1/Q_i$) as a function of the average photon number within the resonator (see Fig. 2 e). Resonators from film A show higher losses across all powers than resonators from film B irrespective of whether they are bare or tunable. Whilst ATune shows more losses than ABare and a greater increase in losses at low power, for film B the losses are approximately equal for BTune and BBare. We therefore attribute the difference in losses in film A to on-chip variation in film quality, as commonly seen in CPW resonators. Losses are dominated by losses associated with the film rather than losses introduced by the SQUID even in the single photon limit. The difference between films could be a result of the small recipe differences such as the HF dip for film B; however, the increased loss at high powers is indicative of increased conductor losses associated with the quality of superconducting films.

A. Tunability

In order to study resonator tuning we examine ATune. Without a lumped element inductor, the tunable SQUID inductance is a greater fraction of the total inductance and so this resonator tunes more in frequency. We first study its behaviour in a small perpendicular magnetic field ($\leq 10 \mu\text{T}$). Fig. 3 a shows a typical field sweep; this reveals the smooth tuning of the resonator towards lower frequencies as magnetic field amplitude is increased. The full range of frequency tuning is found to be ≈ 100 MHz, obtained by changing the applied perpendicular field by $\approx 10 \mu\text{T}$ (see Fig. 3 b) [29]. To analyse this behaviour, we start by assuming a Josephson-like sinusoidal current-phase relationship for the nano-constrictions since the length:width ratio of the constrictions shown in Fig. 1 c is approximately one [30]. We therefore treat the superconducting loop as a DC-SQUID with a flux-tunable inductance [16]

$$L_{\text{SQUID}} = \Phi_0 / [4\pi I_{C0} |\cos f|], \quad (1)$$

where I_{C0} is the zero-field critical current of the SQUID, $f = \pi\Phi/\Phi_0$ is the frustration of the SQUID and Φ_0 is

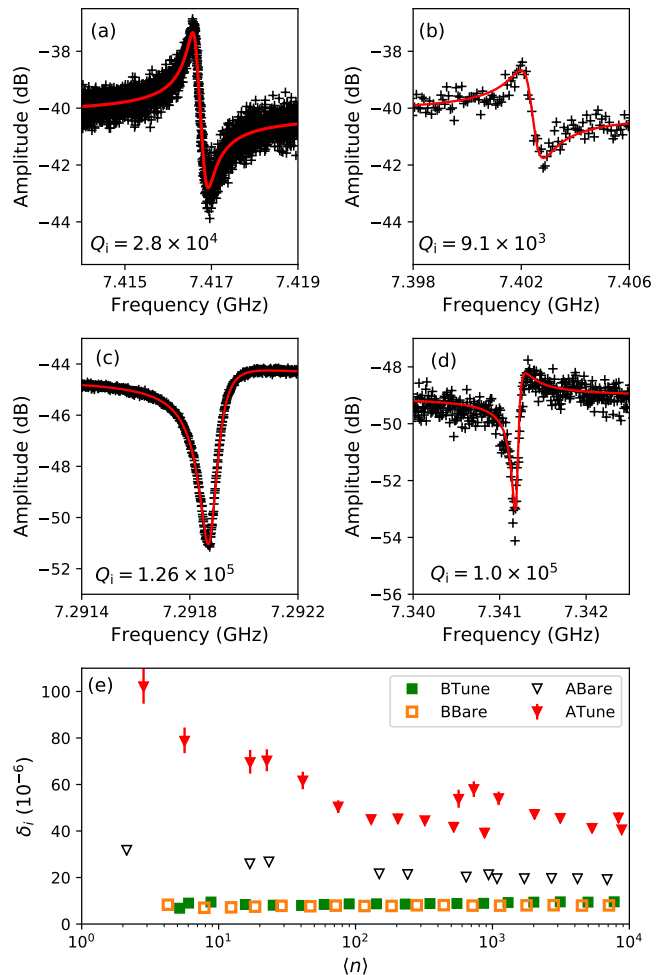


Figure 2. S_{21} amplitude response (black crosses) and fits (red line) for (a, b) ATune and (c, d) BTune. Measurements are performed at (a, c) zero field and (b, d) ~ 0.5 mT applied perpendicular field. All responses are recorded at a power of ~ -106 dBm and internal quality factors are indicated in the figure. The lower frequency of BTune in (c) than in (d) is due to device aging between measurements. The local fields in (b) and (d) are ~ 60 mT and ~ 20 mT respectively. (e) Internal losses of all four resonators as a function of average photon number stored in the resonator. Error bars are shown where they are larger than the markers.

the flux quantum.

The total impedance Z_T of a transmission line terminated by a SQUID is given at frequency ν by

$$Z_T = \frac{Z(Z_{\text{SQUID}} + jZ \tan(2\pi\nu d/v))}{(Z + jZ_{\text{SQUID}} \tan(2\pi\nu d/v))}, \quad (2)$$

where d is the length of the transmission line, Z is the impedance of the transmission line, Z_{SQUID} the impedance of the SQUID and $v = \sqrt{1/l_0 c_0}$ the speed of light in the transmission line where c_0 (l_0) is the capacitance (inductance) per unit length. Z_T is real at resonance and the resonant frequencies ν_i are therefore

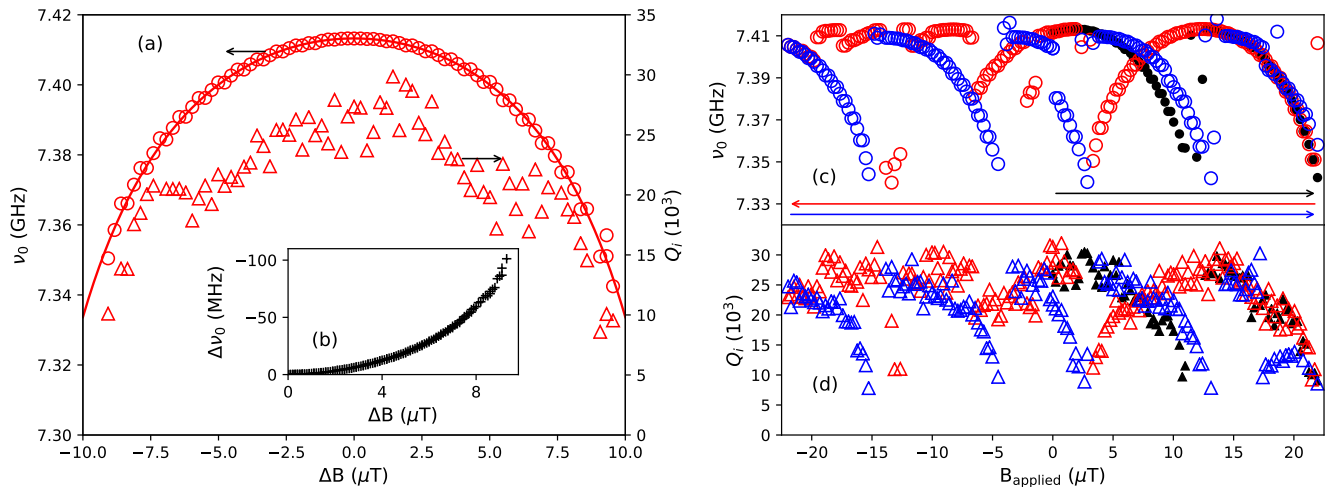


Figure 3. (a) The tuning of resonant frequency (circles) and quality factor (triangles) of ATune as magnetic field is swept. The resonant frequency is fitted by Eq. 5, with fitting parameters $A = 0.050$ and $K = 0.101 \text{ } (\mu\text{T})^{-1}$. For the data shown, the central value $\Delta B = 0$ corresponds to an applied field $B = 12.4 \text{ } \mu\text{T}$. (b) Tuning of the resonator when the field is changed in $0.1 \mu\text{T}$ steps from $B = 12.3 \text{ } \mu\text{T}$. A maximal detuning of the resonator of -101 MHz is obtained. (c) Resonant frequency and (d) internal quality factor of ATune as applied field is swept from 0 to $22 \text{ } \mu\text{T}$ (black), then down from $22 \text{ } \mu\text{T}$ to $-22 \text{ } \mu\text{T}$ (red) and then back up from $-22 \text{ } \mu\text{T}$ to $22 \text{ } \mu\text{T}$ (blue). The sweep directions are shown by arrows at the bottom of (c).

given by

$$\tan\left(\frac{2\pi\nu_i d}{v}\right) = \frac{|Z_T|}{l_0 v}, \quad (3)$$

which may be solved numerically. The fundamental resonant frequency may be expressed approximately [31] in terms of the total inductance L and capacitance C of the distributed resonator:

$$\nu_0(B) = \frac{1}{4\sqrt{(L_{\text{res}} + L_{\text{SQUID}}^0 + \Delta L(B))C}}, \quad (4)$$

where L_{res} is the inductance of the resonator excluding the SQUID, L_{SQUID}^0 is the zero-field inductance of the SQUID. $\Delta L(B)$ is the change of inductance of the SQUID with field which, from Eq. 1, is equal to $\Phi_0/4\pi I_{C0} \times (1/|\cos(f)| - 1)$. Assuming $f \propto B$, an assumption which we examine further below, we can write

$$\frac{\nu_0(B)}{\nu_0(0)} = \sqrt{\frac{1}{1 + \frac{\Delta L(B)}{L_{\text{res}} + L_{\text{SQUID}}^0}}} = \sqrt{\frac{1}{1 - A + \frac{A}{|\cos(KB)|}}}, \quad (5)$$

where $A = \Phi_0/[4\pi I_{C0}(L_{\text{res}} + L_{\text{SQUID}}^0)]$ and $f = KB$ so that K scales field to f . The observed $\nu_0(B)$ dependence of the resonator in Fig. 3 fits well with Eq. 5, allowing determination of A and K .

We next consider the relation between the field periodicity of the tuning behaviour and the flux quantum. SQUID behaviour is periodic in applied flux. The area of the SQUID loop in ATune is $A_{\text{loop}} = 3.7 \pm 0.3 \text{ } \mu\text{m}^2$,

so $10 \text{ } \mu\text{T}$ (the field required to maximally tune the resonator) corresponds to a flux $BA_{\text{loop}} \approx 0.02\Phi_0$. Assuming the tuning arises from the SQUID, the field required to maximally tune the resonator implies that the local flux density at the SQUID is much greater than the $10 \text{ } \mu\text{T}$ applied by the magnet. This indicates substantial flux focusing due to flux expulsion from the superconducting ground plane surrounding the resonators. We return to the topic of flux focusing later.

As ATune is tuned away from ν_0 , Q_i is found to drop from its maximum value, 2.8×10^4 , to 1.0×10^4 when maximally tuned. The same trend of Q_i decreasing with tuning is also seen in BTune. This phenomenon of Q_i decreasing with tuning has previously been observed and attributed to increasing thermal noise as the SQUID is tuned [15] or increased dissipation caused by a sub-gap resistance [16]. An alternative explanation could be that dilute surface spins [32] induce spectral broadening of the resonance lineshape by flux-noise-based frequency jitter in these flux-tunable resonators. However, even for the highest values of flux noise in Ref. 33, which correspond to $\sim 100\mu\Phi_0$, the corresponding frequency jitter would be too small to create sufficient spectral broadening to explain the drop in Q_i observed here. The source of these extra losses is the subject of ongoing work.

B. Hysteresis and Premature Switching

When tuning ATune over more than one period, as shown in Fig. 3c and d, a hysteretic behaviour is seen, similar to that previously reported in Al constriction SQUID resonators [17]. In addition, frequency jumps

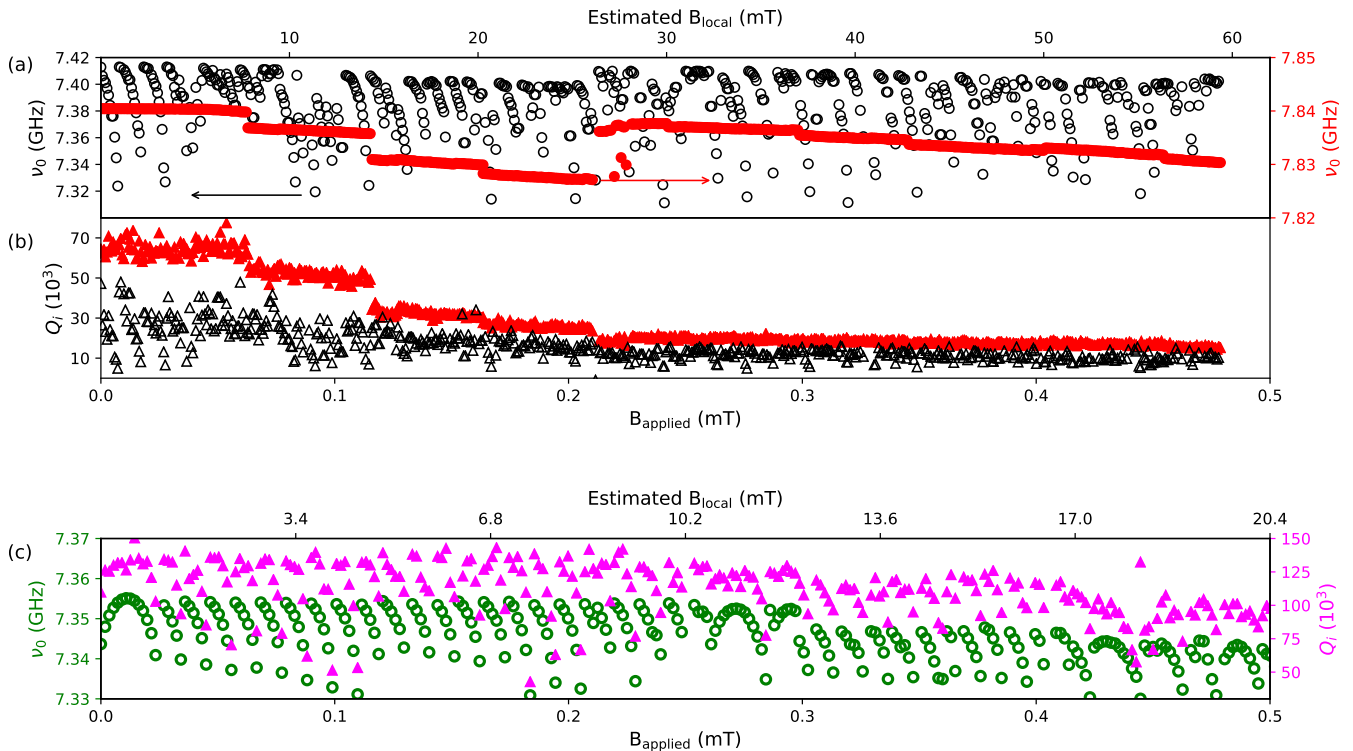


Figure 5. Magnetic-field dependence of (a) resonant frequency and (b) internal quality factor for ATune (black, unfilled symbols) and ABare (red, filled symbols). The local field B_{local} is estimated based on measurements of flux focusing (see main text). (c) Magnetic field dependence of resonant frequency (unfilled green circles) and internal quality factor (magenta triangles) for BTune. Local field is determined as for ATune.

from zero to ≈ 0.5 mT, which corresponds to a local field at the SQUID of ≈ 60 mT for chip A and ≈ 20 mT for chip B due to different flux focusing factors. The smaller size of chip B likely contributes to the smaller flux focusing factor.

The resonance responses and their fits at these fields are shown in Fig. 2b, c. Even at these perpendicular magnetic fields, the internal quality factor of ATune (BTune) is $Q_i = 9.1 \times 10^3$ (9.98×10^4) and the resonator remains tunable, demonstrating the field resilience of these devices. Indeed Fig. 5c shows that BTune retains a high quality factor right across the field range shown, even after tuning through 42 periods.

For ABare, ν_0 and Q_i tune weakly and smoothly as the applied magnetic field is increased up to about 0.21 mT with the exception of abrupt drops in both ν_0 and Q_i at four field values up to 0.2 mT (see Fig. 5). This step-like response of Q_i vs magnetic field is consistent with the formation of vortices on the superconducting resonator's central conductor [37]. For ATune, Q_i modulates by a factor of about 5 with field as the resonator tunes (as previously shown in Fig. 3). In addition to the modulation with tuning, the maximum Q_i also drops with increasing applied field. The magnitude and field scale of this drop are similar to those of the bare resonator. The respective $Q_i(B)$ dependences for ATune

and ABare are consistent with the maximum of the field-modulated Q_i in ATune being limited, as B increases, by the same physics which causes the step-like reductions in Q_i for ABare. The similarity is even more clearly seen in $\nu_0(B)$, where the untuned resonant frequency of ATune jumps up at an applied field of 0.21 mT just as in the bare resonator. This suggests that not only does the nanoSQUID introduce minimal loss at zero applied field, the resonator's field resilience is the limiting factor in the field performance of the device. This is also consistent with measurements of nanoSQUIDs fabricated from ultrathin niobium films successfully operating in parallel fields up to 7 T [38]. Our results are therefore promising for future generations of devices where SQUIDs are embedded within field-resilient resonators. Importantly, ATune operates at local fields comfortably above 30 mT (and BTune looks likely to also operate at such fields), the first clock transition of bismuth spins.

In the literature, resonator tuning is typically given in units of flux quanta. This means that there are no comparable results on field resilience of tunable resonators to which this device can be compared. Therefore, we believe that this study is the first report addressing the field resilience of tunable resonators.

IV. CONCLUSIONS

In conclusion, we have embedded constriction nanoSQUIDs in Nb resonators, and shown that this device geometry results in a frequency tunable resonator with 100 MHz of tuning demonstrated in a 7.42 GHz resonator. We fabricate these devices from two Nb chips and show that the untuned quality factor of these resonators is limited by the bare resonator technology rather than embedding the SQUID, up to internal quality factors of $Q_i = 1.2 \times 10^5$ — the highest quality factor SQUID-tunable resonator reported to date. These results are realised in two different resonators where one has high quality and the other is more tunable, however there is no fundamental trade-off being made between quality and tunability in these devices. By comparing the quality factors of tunable and bare resonators we demonstrate that the quality is determined by the superconducting films. The tunability differs due to different device geometries. We show that even these high quality factors are resonator-limited both at zero-field and applied perpendicular magnetic fields up to 0.5 mT and for resonator photon number from 10^4 down to single photons at zero field. These resonators remain tunable at applied perpendicular fields of 0.5 mT and retain an untuned quality factor $\sim 1 \times 10^5$. The devices presented here compare favourably with the highest quality tunable resonators previously reported [39]. Those resonators tune due to kinetic inductance shifts from DC currents and achieve high-power quality factors of 1.8×10^5 ; there are no reports of low power operation.

A number of modifications to the device and measurement setup may straightforwardly be made to improve field resilience, specifically: operating the device in

parallel fields (which tune spins to the clock transition without applying large fields to the resonator), modifying the device design by the addition of anti-dots [40], patterning the whole ground-plane [41] and/or the use of resonator designs inherently more robust to external field [40–42]. The nanoSQUIDs allow us to measure the local magnetic field around the resonators and we find that the local fields are 30–120 time greater than the applied fields meaning these modifications should straightforwardly significantly improve field resilience.

These resonators hold great promise for future hybrid quantum system applications. For example, a tunable resonator operating at 27mT coupled to Bi spins in Si could address spins at their clock transition. The resonator could be tuned into resonance with the spins, and ESR pulse sequences applied, before the resonator is tuned away from the spins in frequency, allowing the long-coherence-time spins to store quantum information, unperturbed by the resonators.

V. ACKNOWLEDGEMENTS

The authors thank E. J. Romans, A. Blois, S. Probst, P. Bertet, C. W. Zollitsch for useful discussions. This project has received funding from the European Unions Horizon 2020 research and innovation programme under the Marie Skłodowska-Curie grant agreement No 705713 QUINTESENS (E. D.-F.), the European Community’s Seventh Framework Programme through grant agreement No. 279781 (ASCENT) (J.M.), Carl Zeiss Semiconductor Manufacturing (O. W. K.) and the U.K. Engineering and Physical Sciences Research Council, Grant Numbers EP/J017329/1 (J. C. F.), EP/K024701/1 and EP/H005544/1 (O. W. K. and P. A. W.), EP/P510270/1 (O. W. K.).

-
- [1] A Bienfait, JJ Pla, Y Kubo, X Zhou, M Stern, CC Lo, CD Weis, T Schenkel, D Vion, D Esteve, JLL Morton, and P Bertet, Controlling spin relaxation with a cavity, *Nature* **531**, 74 (2016).
 - [2] Y Kubo, FR Ong, Patrice Bertet, Denis Vion, V Jacques, D Zheng, A Dréau, J-F Roch, Alexia Auffèves, Fedor Jelezko, Wrachtrup J, MF Barthe, P Bergonzo, and D Esteve, Strong coupling of a spin ensemble to a superconducting resonator, *Physical Review Letters* **105**, 140502 (2010).
 - [3] S Probst, H Rotzinger, S Wünsch, P Jung, M Jerger, M Siegel, AV Ustinov, and PA Bushev, Anisotropic rare-earth spin ensemble strongly coupled to a superconducting resonator, *Physical Review Letters* **110**, 157001 (2013).
 - [4] H Huebl, CW Zollitsch, J Lotze, F Hocke, M Greifenstein, A Marx, R Gross, and STB Goennenwein, High cooperativity in coupled microwave resonator ferrimagnetic insulator hybrids, *Physical Review Letters* **111**, 127003 (2013).
 - [5] LV Abdurakhimov, S Khan, NA Panjwani, JD Breeze, S Seki, Y Tokura, JLL Morton, and H Kurebayashi, Strong coupling between magnons in a chiral magnetic insulator Cu_2OSeO_3 and microwave cavity photons, arXiv preprint arXiv:1802.07113 (2018).
 - [6] Xiao Mi, JV Cady, DM Zajac, PW Deelman, and JR Petta, Strong coupling of a single electron in silicon to a microwave photon, *Science* **355**, 156–158 (2017).
 - [7] C Grèzes, Y Kubo, B Julsgaard, T Umeda, J Isoya, H Sumiya, H Abe, S Onoda, T Ohshima, K Nakamura, I Diniz, A Auffèves, V Jacques, J-F Roch, D Vion, D Esteve, K Moelmer, and P Bertet, Towards a spin-ensemble quantum memory for superconducting qubits, *Comptes Rendus Physique* **17**, 693–704 (2016).
 - [8] TW Larsen, KD Petersson, F Kuemmeth, TS Jespersen, P Krogstrup, J Nygård, and CM Marcus, Semiconductor-nanowire-based superconducting qubit, *Physical Review Letters* **115**, 127001 (2015).
 - [9] F Yan, S Gustavsson, A Kamal, J Birenbaum, AP Sears, D Hover, TJ Gudmundsen, D Rosenberg, G Samach, S Weber, JL Yoder, TP Orlando, J Clarke, AJ Kerman, and WD Oliver, The flux qubit revisited to enhance coherence and reproducibility, *Nature Communications* **7**, 12964 (2016).

- [10] A Dunsworth, A Megrant, C Quintana, Z Chen, R Barends, B Burkett, B Foxen, Y Chen, B Chiaro, A Fowler, R Graff, E Jeffrey, J Kelly, E Lucero, JY Mutus, M Neeley, C Neill, P Roushan, D Sank, A Vainsencher, J Wenner, TC White, and JM Martinis, Characterization and reduction of capacitive loss induced by sub-micron josephson junction fabrication in superconducting qubits, *Applied Physics Letters* **111**, 022601 (2017).
- [11] S Blum, C O'Brien, N Lauk, P Bushev, M Fleischhauer, and G Morigi, Interfacing microwave qubits and optical photons via spin ensembles, *Physical Review A* **91**, 033834 (2015).
- [12] J Burnett, L Faoro, I Wisby, VL Gurtovoi, AV Chernykh, GM Mikhailov, VA Tulin, R Shaikhaidarov, V Antonov, PJ Meeson, AY Tzalenchuk, and T Lindström, Evidence for interacting two-level systems from the $1/f$ noise of a superconducting resonator, *Nature Communications* **5**, 4119 (2014).
- [13] R Barends, J Kelly, A Megrant, A Veitia, D Sank, E Jeffrey, TC White, J Mutus, AG Fowler, B Campbell, Y Chen, Z Chen, B Chiaro, A Dunsworth, C Neill, P O'Malley, P Roushan, A Vainsencher, J Wenner, AN Korotkov, Cleland AN, and JM Martinis, Superconducting quantum circuits at the surface code threshold for fault tolerance, *Nature* **508**, 500–503 (2014).
- [14] A Megrant, C Neill, R Barends, B Chiaro, Yu Chen, L Feigl, J Kelly, Erik Lucero, Matteo Mariantoni, PJJ O'Malley, D Sank, A Vainsencher, J Wenner, TC White, Y Yin, J Zhao, Palmström CJ, John M Martinis, and AN Cleland, Planar superconducting resonators with internal quality factors above one million, *Applied Physics Letters* **100**, 113510 (2012).
- [15] A Palacios-Laloy, F Nguyen, F Mallet, P Bertet, D Vion, and D Esteve, Tunable resonators for quantum circuits, *Journal of Low Temperature Physics* **151**, 1034–1042 (2008).
- [16] M Sandberg, CM Wilson, F Persson, T Bauch, G Johansson, V Shumeiko, T Duty, and P Delsing, Tuning the field in a microwave resonator faster than the photon lifetime, *Applied Physics Letters* **92**, 203501 (2008).
- [17] EM Levenson-Falk, R Vijay, and I Siddiqi, Nonlinear microwave response of aluminum weak-link josephson oscillators, *Applied Physics Letters* **98**, 3115 (2011).
- [18] AA Adamyman, SE Kubatkin, and AV Danilov, Tunable superconducting microstrip resonators, *Applied Physics Letters* **108**, 172601 (2016).
- [19] AT Asfaw, AJ Sigillito, AM Tyryshkin, T Schenkel, and SA Lyon, Multi-frequency spin manipulation using rapidly tunable superconducting coplanar waveguide microresonators, *Applied Physics Letters* **111**, 032601 (2017).
- [20] C Granata and A Vettoliere, Nano superconducting quantum interference device: A powerful tool for nanoscale investigations, *Physics Reports* **614**, 1–69 (2016).
- [21] MJ Martínez-Pérez, R Kleiner, and D Koelle, NanoSQUIDs Applied to the Investigation of Small Magnetic Systems, in *The Oxford Handbook of Small Superconductors* (OUP, 2017).
- [22] T Schwarz, J Nagel, R Wölbing, M Kemmler, R Kleiner, and D Koelle, Low-noise nano superconducting quantum interference device operating in tesla magnetic fields, *ACS Nano* **7**, 844–850 (2013).
- [23] L Hao, D C Cox, and J C Gallop, Characteristics of focused ion beam nanoscale josephson devices, *Superconductor Science and Technology* **22**, 064011 (2009).
- [24] MD Jenkins, U Naether, M Ciria, J Sesé, J Atkinson, C Sánchez-Azqueta, E del Barco, J Majer, D Zueco, and F Luis, Nanoscale constrictions in superconducting coplanar waveguide resonators, *Applied Physics Letters* **105**, 162601 (2014).
- [25] J Burnett, J Sagar, OW Kennedy, PA Warburton, and JC Fenton, Low-loss superconducting nanowire circuits using a neon focused ion beam, *Physical Review Applied* **8**, 014039 (2017).
- [26] R Meservey and BB Schwartz, *Equilibrium properties: Comparison of experimental results with predictions of the BCS theory*, Tech. Rep. (Massachusetts Inst. of Tech., Cambridge, 1969).
- [27] See Supplemental Material at ... for details on further statistics on junction dimensions, measurements on additional devices and calculations of resonator and SQUID inductance. .
- [28] S Probst, FB Song, PA Bushev, AV Ustinov, and M Weides, Efficient and robust analysis of complex scattering data under noise in microwave resonators, *Review of Scientific Instruments* **86**, 024706 (2015).
- [29] Here, field has been changed in small (0.1 μ T) steps to approach maximal detuning whilst ensuring that the point of maximal detuning is not overshoot before the sweep direction is reversed.
- [30] AA Golubov, MY Kupriyanov, and E Il'ichev, The current-phase relation in josephson junctions, *Reviews of modern physics* **76**, 411 (2004).
- [31] PJ Jones, JAM Huhtamäki, J Salmilehto, KY Tan, and M Möttönen, Tunable electromagnetic environment for superconducting quantum bits, *Scientific Reports* **3**, 1987 (2013).
- [32] SE de Graaf, AA Adamyman, T Lindström, D Erts, SE Kubatkin, AY Tzalenchuk, and AV Danilov, Direct Identification of Dilute Surface Spins on Al_2O_3 : Origin of Flux Noise in Quantum Circuits, *Physical Review Letters* **118**, 057703 (2017).
- [33] G Ithier, E Collin, P Joyez, PJ Meeson, D Vion, D Esteve, F Chiarello, A Shnirman, Y Makhlin, J Schrieffer, and G Schön, Decoherence in a superconducting quantum bit circuit, *Physical Review B* **72**, 134519 (2005).
- [34] M Tinkham, *Introduction to superconductivity* (Courier Corporation, 2004).
- [35] Daniel Bothner, Dominik Wiedmaier, Benedikt Ferdinand, Reinhold Kleiner, and Dieter Koelle, Improving superconducting resonators in magnetic fields by reduced field focussing and engineered flux screening, *Physical Review Applied* **8**, 034025 (2017).
- [36] Eun-jong Kim, JR Johansson, and Franco Nori, Circuit analog of quadratic optomechanics, *Physical Review A* **91**, 033835 (2015).
- [37] I. Nsanzeineza and B. L. T. Plourde, Trapping a single vortex and reducing quasiparticles in a superconducting resonator, *Physical Review Letters* **113**, 117002 (2014).
- [38] Lei Chen, Wolfgang Wernsdorfer, Christos Lampropoulos, George Christou, and Irinel Chiorescu, On-chip SQUID measurements in the presence of high magnetic fields, *Nanotechnology* **21**, 405504 (2010).
- [39] Michael R Vissers, Johannes Hubmayr, Martin Sandberg, Saptarshi Chaudhuri, Clint Bockstiegel, and Jiansong Gao, Frequency-tunable superconducting resonators

- via nonlinear kinetic inductance, *Applied Physics Letters* **107**, 062601 (2015).
- [40] D Bothner, T Gaber, M Kemmler, D Koelle, and R Kleiner, Improving the performance of superconducting microwave resonators in magnetic fields, *Applied Physics Letters* **98**, 102504 (2011).
- [41] SE de Graaf, AV Danilov, Astghik Adamyan, Thilo Bauch, and SE Kubatkin, Magnetic field resilient superconducting fractal resonators for coupling to free spins, *Journal of Applied Physics* **112**, 123905 (2012).
- [42] N Samkharadze, A Bruno, P Scarlino, G Zheng, DP DiVincenzo, L DiCarlo, and LMK Vandersypen, High-kinetic-inductance superconducting nanowire resonators for circuit qed in a magnetic field, *Physical Review Applied* **5**, 044004 (2016).